Horseradish Peroxidase Oxidation of Tyrosine-Containing Peptides and Their Subsequent Polymerization: A Kinetic Study†

Thierry Michon,*,‡ Michel Chenu,‡ Nicolas Kellershon,§ Michel Desmadril,|| and Jacques Guéguen‡

Unité de Biochimie et de Technologie des Protéines, INRA rue de la Géraudière, BP 1627, 44316 Nantes, France, Institut Jacques Monod, tour 43, Université Paris VII, 2 place Jussieu, 75251 Paris cedex 05, France, and EPCM, Bat. 430, Université Paris Sud, 91405 Orsay Cedex, France

Received December 27, 1996; Revised Manuscript Received April 7, 1997⊗

ABSTRACT: Tyrosine-containing model peptides were oxidized by horseradish peroxidase (HRP). This led to a peptide polymerization via condensation of the aromatic rings. Dimers, trimers, and tetramers (depending on the peptide length and on the position of the tyrosine in the sequence) were identified by electron spray mass spectroscopy. The second-order rate constants of the second step of the HRP reduction (CII → E) was decreased by the presence of a positively charged amino group in the vicinity of the aromatic ring as determined by stopped flow measurements [$k_3 = 19\,398\ M^{-1}\ s^{-1}$ and $k_3 = 1016\ M^{-1}\ s^{-1}$ for *N*-acetyltyrosine (NAT) and L-Tyr oxidations, respectively]. High-performance liquid chromatography was used to follow the kinetics of polymerization of some model peptides after their enzymatic oxidation. The first polymerization products exhibited a strong inhibitory effect toward further oxidation by HRP. This effect was not observed when using manganese-dependent peroxidase (MnP) which does not bind directly to the tyrosine residue but rather acts as a "distant catalyst". Saturation of the HRP was achieved with Pro-Gln-Gln-Pro-Tyr ($k_{cat} = 58\ s^{-1}$, $K_M^{app} = 2.1$ mM), NAT ($k_{cat} = 94\ s^{-1}$, $K_M^{app} = 5.6$ mM), and Gly-Tyr ($k_{cat} = 175\ s^{-1}$, $K_M^{app} = 10.8$ mM). Analysis of steady state kinetics of the reaction showed that the dimers formed initially behaved like competitive inhibitors. The value of the dissociation constant between HRP and dimers was 20 μM. A simplified model which accounts for these observations, including the formation of a Michaelis−Menten-like complex involving the donor and enzyme, is proposed and discussed.

It has been reported that peroxidases are involved in the post-translational maturation of proteins. Resilin, a protein which is present in the cuticle of insects and arthropods, forms a network through intermolecular dityrosine bonds (Andersen, 1966) (Figure 1A). Tyrosine−tyrosine cross-linking has also been found between molecules of elastin (Labella et al., 1967). In the plant kingdom, peroxidases are involved in the building of the cell wall (Federico & Angelini, 1986) and in the repair process after injuries (Scalet et al., 1991). *In vivo*, peroxidase oxidations induce the reticulation of extensin, a major protein of the cell wall, through isodityrosine bonds (Figure 1B). However, *in vitro*, it has not yet been possible to enzymatically catalyze this type of bond (Fry, 1982). The yields of the *in vitro* reticulation of several proteins subsequent to their oxidation by HRP[1] have been compared (Amado et al., 1984). More recently, the dimerization of calmodulin via the formation of a dityrosine bridge catalyzed by peroxidases was analyzed in detail (Malencik & Anderson, 1996). In proteins, the degree of polymerization is generally limited to dityrosines,

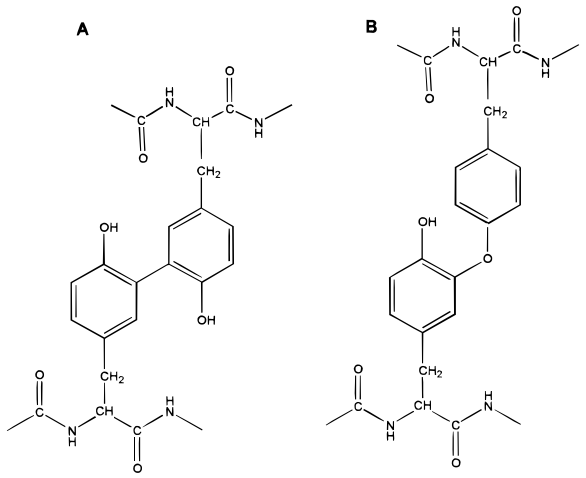

FIGURE 1: Schematic structures of dityrosine (A) and isodityrosine (B).

trityrosine formation being subjected to steric hindrance. In contrast, trityrosines have been detected in resilin (Andersen, 1966). Several studies dealing with the kinetics of dityrosine formation after free tyrosine oxidation by HRP have already been published (Bayse et al., 1972; Ralston & Dunford, 1978; Ralston & Dunford, 1980). In the presence of hydrogen peroxide, HRP catalyzes the formation of an unstable free radical on the aromatic ring of the tyrosine side chain. The enzyme reduces one molecule of H_2O_2 while oxidizing two tyrosine molecules. The free radicals condense rapidly compared to their rate of formation by the peroxidase. A C−C bond is formed at the ortho positions with respect to the phenol groups. Upon further oxidation, dityrosine may

† This work was supported in part by La Région des Pays de La Loire.

* To whom correspondence should be addressed. Telephone: 33-02-40-67-50-59. Fax: 33-02-40-67-50-25. E-mail: michon@nantes.inra.fr.

‡ Unité de Biochimie et de Technologie des Protéines.

§ Université Paris VII.

|| Université Paris Sud.

⊗ Abstract published in *Advance ACS Abstracts*, June 15, 1997.

[1] Abbreviations: HRP, horseradish peroxidase; MnP, manganese peroxidase; NAT, *N*-acetyltyrosine; NATA, *N*-acetyltyrosine amide; TFA, trifluoroacetic acid; *py*, Pro-Gln-Gln-Pro-Tyr; *yp*, Tyr-Pro-Gln-Gln-Pro-Ala; *pyp*, Pro-Gln-Gln-Pro-Tyr-Pro-Gln-Gln-Pro-Ala; *pyq*, Gln-Gln-Met-Gln-Gln-Ser-Pro-Arg-Ser-Thr-Arg-Pro-Tyr-Gln-Gln-Arg-Pro-Gly-Gln-Gln.

S0006-2960(96)03168-6 CCC: $14.00

condense with other tyrosines to form polymers of higher degrees. The studies dealing with the oxidation of tyrosines and their ensuing polymerization generally postulate that during the time of observation only dimers are formed. Nevertheless, it is generally not taken into account that the measured signal (often an increase in absorption or fluorescence) results from differing contributions of various tyrosine polymers. The analysis of products (especially in the case of free tyrosine polymerization) shows that the degree of polymerization proceeds far beyond dityrosine formation (see below). The kinetic constants of dityrosine oxidation by the myeloperoxidase have recently been published (Marquez & Dunford, 1995). However, to our knowledge, a kinetic study including the peroxidative oxidation of peptide-containing tyrosine and the subsequent polymerization of the oxidation products has not been published. The size of the peptidic substrate, the ionic charges around the targeted tyrosine, and its position in the peptide are various factors which should affect the efficiency and the degree of the polymerization. In the plant extracellular matrix, extensin undergoes post-translational cross-linking involving tyrosine included in specific proline rich peptidic motifs [see for review Kieliszewski et al. (1994)]. Model peptides mimicking this type of sequence have been designed. Their enzymatic oxidation and their subsequent polymerization have been investigated.

Four aspects of the peroxidase-induced polymerization are reported in this study. (I) The polymerization products of various tyrosine-containing model molecules obtained after their oxidation by peroxidases have been identified. (II) The overall nonequilibrium kinetics of the polymerization process have been analyzed after oxidation of the substrates by two peroxidases (HRP and MnP) which exhibit different mechanisms. (III) The steady state kinetics of polymerization have also been analyzed. The influence of the initial reaction products on further oxidation by the horseradish peroxidase has been assessed. (IV) The second-order constants of substrate oxidation by HRP have also been determined by fast kinetic measurements. A minimum model is proposed which accounts for our observations.

MATERIALS AND METHODS

Reagents. NATA, NAT, L-Tyr, Gly-Tyr, horseradish peroxidase (type VIA), Blue 2-cross-linked Agarose, and H_2O_2 were purchased from Sigma Chemical Co. Lactic acid, sodium chloride, boric acid, trifluoroacetic acid (TFA), acetonitrile, sodium metabisulfite, sodium and potassium phosphate, sodium tartrate, hydrochloric acid, and manganese sulfate were obtained from Merck Co. and were of the best grade available. Distilled water was further purified using a Milli-Q Millipore system. All buffers and solutions were filtered through a 0.22 μm membrane before use.

Purification of the Mn-Dependent Peroxidase (MnP) from Phanerochaete chrysosporium. The culture medium was a generous gift of M. Asther. Cultures were made in conditions optimized for high enzyme production (Capdevila et al., 1989). MnP was purified using a combination of the methods from Asther et al. (1992) and Glenn et al. (1985). After filtration through a 0.45 μm membrane, the culture medium (50 mL) was loaded onto a DEAE-Sepharose fast flow (1 $\times$ 10 cm) Pharmacia column, previously equilibrated with a mixture of 15 mM sodium phosphate and 20 mM sodium tartrate at pH 6.5. Under these conditions, the anionic hemoproteins were not retained in the dead volume of the column. This fraction which was enriched in peroxidase activities was recovered and loaded onto a Q Sepharose fast flow Pharmacia column equilibrated in the same buffer. A 0 to 300 mM NaCl gradient was applied over 30 min to the column. The material which absorbed at 410 nm was collected into three fractions. The first fraction contained the lignin peroxidase isoforms H1 and H2 and the Mn peroxidase isoforms H3 and H4. This fraction was dialyzed against 50 mM sodium succinate at pH 4.5. It was loaded onto a Blue Agarose (1 $\times$ 10 cm) column. The proteins were eluted with a 0 to 300 mM NaCl gradient. The fractions which absorbed at 410 nm were collected and identified using an FPLC (Pharmacia) analytic chromatographic system equipped with a mono Q column (Kirk et al., 1986). Isoform H4 of the MnP was used for the kinetic experiments. The A_{406}/A_{280} ratio (RZ) of the purified enzyme was around 3.8−4. The enzyme concentrations were estimated using a molar extinction coefficient of 127×10^3 M^{-1} cm^{-1} (Millis et al., 1989). The enzymatic preparations were unstable (80% decrease after 72 h at 4 °C) and were used immediately.

Enzymatic Activities. The activities were routinely determined by following the formation of $(NAT)_2$ at the steady state using H_2O_2 and NAT as the acceptor and donor, respectively. In order to compare the activities of the MnP and HRP, measurements were made in 50 mM sodium lactate and 0.1 mM $MnSO_4$ containing 2.5 mM NAT. The reaction was initiated by the introduction of H_2O_2 at a final concentration of 0.25 mM. The kinetics of polymerization of NAT were followed by the increase in absorbance at 293 nm ($\epsilon_{293}^{4.5} = 4488$ M^{-1} cm^{-1}). Under these conditions, the increase in absorbance was linear over a period of 2 min. The specific activities were 27 UE (400 nkat) and 3.5 UE (51 nkat) per milligram of enzyme for HRP and MnP, respectively. The specific activity of HRP was also measured at 318 nm ($\epsilon_{318}^{8.7} = 3627$ cm^{-1} M^{-1}) in 50 mM phosphate buffer at pH 8.7. The activities were 135 UE/mg (2 μkat) with 0.25 mM H_2O_2 and 350 UE/mg (5.2 μkat) with 0.1 mM H_2O_2 (1 UE is the amount of enzyme which catalyzes the transformation of 1 μmol of substrate per minute under defined conditions; 1 kat is the amount of activity sufficient to catalyze the transformation of 1 mol of substrate into products in 1 s under standard conditions).

HRP Oxidation of Tyrosine-Containing Model Molecules. Model peptides (*py*, *yp*, *pyp*, and *pyq* each at 0.5 mM) were dissolved in 50 mM ammonium acetate at pH 8.7. HRP was added (final concentration of 0.5 μM) to the peptide solutions, and the reaction was started by the addition of 2 mM H_2O_2. The reaction was allowed to proceed at 37 °C in the dark for 24 h. The products were than characterized as described in Purification and Analysis of the Polymerization Products.

Purification of Di-N-acetyltyrosine. A volume of 500 mL of a 20 mM NAT solution in 0.2 M borate buffer at pH 9 was incubated with 1 μM HRP at 37 °C in the dark under gentle steering. In order to prevent peroxidase inhibition at high peroxide concentrations, H_2O_2 was pumped into the mixture from a 100 mM stock solution (flow rate of 5 mL/h). After 24 h, the reaction was stopped by addition of sodium metabisulfite. The pH was adjusted to 2.5 with concentrated HCl. The mixture was separated on a G10 Sephadex column (Pharmacia) equilibrated in water. The products were separated under three peaks absorbing at 275

nm. Fractions were collected and their contents analyzed by RP-HPLC/ESI-MS. Samples exhibiting a high degree of polymerization were eluted in the void volume. Samples corresponding to peak 2 contained $(NAT)_2$ with traces of trimers and tetramers. Samples corresponding to peak 3 contained dimer and monomer. Peak 2 isolate was freeze-dried and stored at −20 °C. For kinetic experiments, the $(NAT)_2$ isolate was purified further from this fraction using HPLC.

Purification and Analysis of the Polymerization Products. A C18 LiChroCART 250-4 Superspher (0.4 × 25 cm, porosity of 100 Å) column (Merck, Darmstadt, Germany) was equilibrated in 80% medium A containing 0.06% TFA in water and 20% medium B containing 50% acetonitrile and 0.04% TFA in water. The samples were injected onto the column, and after a 5 min wash, a 20 to 50% B gradient was applied over 15 min, at a flow rate of 1 mL/min. This gradient was used to separate all the major compounds obtained after peroxidase oxidation. A mass spectrometer was coupled on-line with the HPLC system in order to analyze the eluted compounds (RP-HPLC/ESI-MS). The electrospray mass spectrometer (APII 5Sciex, Thornhill, Ontario, Canada) was a single quadrupole equipped with an atmospheric pressure ionization ion source. The sample was delivered to the sprayer unit by a 1/8 splitting of the RP-HPLC flux, and sprayed at 55 °C, through a stainless steel capillary held at a high voltage between 4.5 and 5.2 kV. The liquid nebulization was aided by a coaxial air flow along the sprayer, adjusted between 0.3 and 0.4 MPa. The interface between the sprayer and the mass analyzer consisted of a conical orifice with a 100 μm inside diameter. The potential of the orifice was 70 V. The instrument was calibrated with ammonium adduct ions of polypropylene glycols (PPG). The unit resolution was maintained across the whole mass range for singly charged PPG calibrations, according to the 55% valley definition. Each scan was acquired over a range of mass-to-charge (m/z) values of 300−2000 (u) using a step size of 0.33 Da. Molecular masses were determined from the measured m/z values for the protonated molecules. Data were acquired on an Apple Macintosh computer and were processed using software package Tune 2.2 and Mac Spec 3.2 (Sciex).

Determination of Molar Extinction Coefficients of the Polymers. After purification of the polymers using reverse phase chromatography, the purity was checked against mass spectroscopy analysis. The products were solubilized at various pH values, and absorption spectra were recorded. Aliquots from these solutions were hydrolyzed under vacuum in a 6 N HCl gas phase at 110 °C for 24, 48, and 72 h (1 mM phenol was added in the sample to prevent acidic degradation of tyrosines). After conversion in phenylthiocarbamyl derivatives, the amino acids were separated and quantified according to the method of Bidlingmeyer et al. (1984). Every sample was analyzed in duplicate in the presence of tyrosine, proline, and glutamic acid as internal standards (recovery of 70, 92, and 98%, respectively, after 24 h of hydrolysis). As the degree of polymerization of the compounds was known (mass spectroscopy determinations), it was possible to determine the molar concentration of the various samples and hence to deduce their molar extinction coefficients.

Further Characterization of the Reaction Products. Absorption and fluorescence spectra of the polymers exhibited the characteristic spectral properties of polytyrosines. All the absorption spectra were recorded using a Cary13E model spectrophotometer (Varian, Australia). The fluorescence spectra were obtained with a SLM-Aminco 4800 spectrofluorimeter.

Analysis of the Kinetics of Polymerization. The appearance of the various polymerization products as a function of time was monitored using the HPLC system and the conditions of elution as described above. Assays were made using monomer concentrations varying in strength from 100 μM to 2 mM. The HRP oxidation was performed in 20 mM ammonium acetate at pH 8.7. The MnP oxidation was performed in a 50 mM sodium lactate solution (pH 4.5) containing 0.1 mM $MnSO_4$. An equivalent amount of MnP and HRP enzyme units had been added in the medium so that it was possible to compare the polymerization kinetics induced by both enzymes. The reaction was initiated by introduction of H_2O_2 in the mixture. The reaction was carried out at 37 °C in the dark. At different time intervals, 100 μL of the mixture was retrieved and the reaction was stopped by adding 100 μL of a mixture containing 10% acetonitrile and 1% TFA in water. The samples were then stored at −20 °C prior to their chromatographic analysis. The relative amounts of the different polymers formed were quantified by integration of the peaks. The true concentrations were determined by means of the experimentally determined extinction coefficients (see above).

Steady State Kinetic Measurements of the Polymerization. Let us consider the overall reaction scheme:

$$E + H_2O_2 \xrightarrow{k_1} CI$$

$$CI + R{-}Tyr \xrightarrow{k_2} CII + R{-}Tyr^{\bullet}$$

$$CII + R{-}Tyr \xrightarrow{k_3} E + (R{-}Tyr)^{\bullet}$$

$$2R{-}Tyr^{\bullet} \xrightarrow{k_4} (R{-}Tyr)_2$$

with CI and CII being compound I and compound II, respectively. The aromatic ring condensation proceeds rapidly. This reaction is not rate-limiting, and k_4 cannot be determined easily. In the scheme above, it is assumed that the stoichiometry of the oxidation is two molecules of donor for one molecule of H_2O_2. In order to validate this model, ''single-turnover'' reductions of CI by various donors were performed as follows. HRP (5 μM) was mixed with H_2O_2 (5.2 μM) to prepare compound I. An equal amount of donor was added. The conversion of compound I to compound II was monitored following the increase of absorbance at 422 nm. For the peptides tested (*py* and *pyp*), the absorbance value remained constant over more than 20 min. In the case of NAT and Gly-Tyr, the absorbance decreased slowly (20% in 30 min), indicating a possible reduction of compound II by the dimers formed. In every case, when an excess of 2 equiv of donor was added, the absorbance decreased and reached the value previously observed for the resting enzyme (data not shown). Thus, it was ascertained in the cases of the model peptides used in this study that the stoichiometry of the reaction was two molecules of donor oxidized for one molecule of H_2O_2.

According to the scheme above, the equation rate of donor oxidation is

$$\frac{d[(R-Tyr)_2]}{dt} = \frac{[E]_{tot}}{\frac{1}{k_1[H_2O_2]} + \frac{1}{k_2[R-Tyr]} + \frac{1}{k_3[R-Tyr]}} \quad (1)$$

It was previously reported that, between pH 5 and 10, the value of k_1, the true second-order rate of formation of compound I (CI), is about 1.6×10^7 M^{-1} s^{-1} (Job & Dunford, 1978). Our determination according to the same method was $(1.9 \pm 0.3) \times 10^7$ M^{-1} s^{-1}. Taking into account the values obtained for k_2 and k_3 (see Table 3) and by choosing adapted concentrations of donor and peroxide, we reduced eq 1 to

$$\frac{d[(R-Tyr)_2]}{dt} = [E]_{tot} k'_4 [R-Tyr] \quad (2)$$

where $k'_4 = (k_2k_3)/(k_2 + k_3)$, $[E]_{tot}$ is the peroxidase concentration, and [R−Tyr] is the concentration of the donor. For all the steady state measurements, the peroxide concentration was set at 100 μM in such a way that eq 2 can be applied. The polymer formation was monitored by a direct recording of the absorbance increase at 318 nm (ΔA) as a function of time. As the lifetime of the free radicals is short, the rate of this increase corresponds to the rate of release of the free radicals by the enzyme. Whatever the phenolic substrate tested, under the conditions used this increase was linear for at least 1 min. The molar extinction coefficient of dityrosine at pH 8.7 and 318 nm was used as in the early part of the reaction the main contribution to the absorbance increase was due to dimer formation. Typically, the reaction mixture contained 2−10 nM HRP, 100 μM H_2O_2, and donor at various concentrations in 50 mM ammonium acetate at pH 8.7 and 20 °C. k'_4 was determined by measuring the rate of dimerization

$$v_0 = \frac{\Delta A}{\Delta t} \frac{1}{[E]_{tot}} \frac{1}{3624} = k'_4 [R-Tyr]_0 \quad (3)$$

with $[R-Tyr]_0$ the initial concentration of the donor. For donor concentrations between 100 and 500 μM, v_0 increased linearly as a function of the donor concentration with a slope equal to k'_4. For some substrates tested, above concentrations of 500 μM, the kinetics were no longer pseudo-first-order and a saturation phenomenon was observed. In these cases, apparent kinetic parameters K_M^{app} and V_m^{app} were determined by fitting the v_0 experimental values to the Michaelis−Menten equation and to its modified form for competitive inhibition in the case of product inhibitions obtained with $(NAT)_2$ (see below).

Fast Kinetics Measurements. The measurements were performed using a SFM3 stopped flow model (Biologic, France) equipped with a monochromator and two photomultipliers. The mechanical subsystem consists of three syringes, two mixing chambers, and an observation chamber. The whole apparatus is inclosed in a water jacket to allow temperature regulation of the reaction chambers. The SFM3 syringes are controlled by a Biologic MPS5 microprocessor power supply. Kinetic data were accumulated on a microcomputer, the dead time of the apparatus being 4 ms. The acquisition time was chosen in order to fit the observed intermediate step. It was set between 100 and 500 ms for the relaxation CI → CII and between 500 ms and 20 s for the relaxation CII → E. The enzyme and H_2O_2 were initially mixed at the same concentration in the first chamber. This CI complex solution, aged for 2 s, was then mixed in the second chamber with various amounts of a concentrated donor stock solution. Absorbance values were obtained at 422 nm from the ratio of the intensity of the transmitted light to that of the reference beam. Pseudo-first-order rate constants (k_i^{obs}) were determined using a nonlinear regression program based on the Marquardt algorithm (Press et al., 1986). The true second-order rate constants k_2 and k_3 were obtained from the slopes of the plots of k_i^{obs} versus donor concentration as $k_i^{obs} = k_i[R-Tyr]_0$. For donor concentrations ranging from 80 to 250 μM for enzymes and H_2O_2 concentrations between 4 and 10 μM, the amplitude of the signal ranged from 0.16 to 0.3 absorbance unit.

RESULTS

Characterization of the Polymers Obtained after Horseradish Peroxidase Oxidation of Model Peptides. The reaction products which absorbed at 275 nm were fractionated by reverse phase chromatography. The molecular masses of the compounds contained in these fractions were analyzed by mass spectroscopy (positive mode detection). The oxidation products of all the tested molecules (with the exception of *pyq*, NAT, and NATA) were distributed between ionic species corresponding to the ionization state of the amino group carried by the N-terminal proline. The mass spectral analysis of the products obtained from *pyq* oxidation revealed a partial conversion of methionine residues into methionine sulfones. The different ionization states of the three arginine residues of the peptide increased the number of possible cationic species. Two species were separated by reverse phase chromatography. The monomer (MW of 2429.5 Da) was distributed as a two-charge species ($m/z = 1215.77$), a three-charge species ($m/z = 810.85$), and a four-charge one ($m/z = 608.3$). A dimer (MW of 4857 Da) was eluted after the monomer. It was distributed as three different ionic species ($m/z = 1620$ for three positive charges, $m/z = 1215.42$ for four positive charges, and $m/z = 972.54$ for five positive charges).

As an example, the analysis of the products obtained from *py* oxidation is shown in Figure 2. The oxidation products were separated in three major fractions (Figure 2A). Fraction I contained only one monoprotonated molecular species ($m/z = 632.3$) (Figure 2B). The determined mass (MW of 631 Da) corresponds to one of the nonoxidized *py* peptides. The retention time of this compound was the same as the *py* one before enzymic treatment. A pure compound was eluted under fraction II. The corresponding mass spectrum showed that this compound was distributed as two ionic species, $m/z = 1261.6$ and $m/z = 631.3$, carrying one and two protons, respectively. The determined mass of 1260 Da allowed us to identify the product as a $(py)_2$ dimer. Fraction III contained two ionic forms of a unique compound. One was biprotonated ($m/z = 946.5$) and the other triprotonated ($m/z = 631.3$). The mass of this compound (MW of 1891 Da) was congruous with a $(py)_3$ trimer. A $(py)_4$ tetramer (MW of 2520 Da) distributed between two ionic states (a biprotonated one, $m/z = 1262$, and a triprotonated one, $m/z = 841.2$) was detected under fraction IV at a low amount

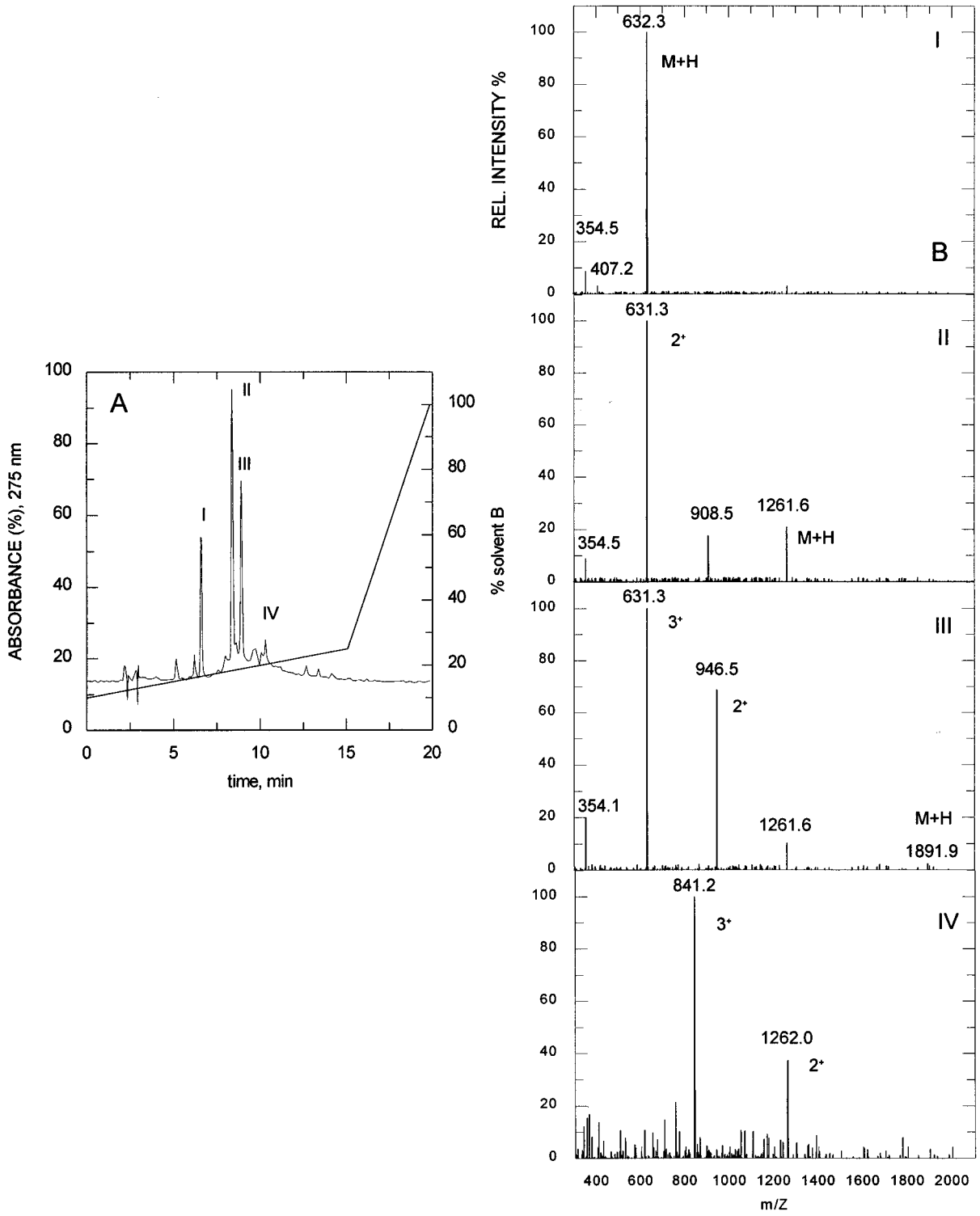

FIGURE 2: (A) Reverse phase separation of the products obtained after a 10 min oxidation of *py* by HRP. The sample containing 0.5 mM *py* was incubated with 2 mM H_2O_2 and 0.6 μM HRP in 50 mM sodium acetate at pH 8.7 for 10 min at 37 °C in the dark. A 250 μL aliquot was withdrawn and diluted twice with 0.1% TFA. Fifty microliters was injected up to the column, and the separation run was performed as described in Materials and Methods. (B) Mass spectra of the material eluted under fractions I−IV. The apparatus was switched on to the positive mode for cation detection. The number of positive charges carried by the different ionic species have been indicated beside the corresponding peaks.

relative to those of the other polymers obtained. The different polymers obtained from the tested model substrates and their respective yield are summarized in Table 1. The degree of polymerization obtained would seem to be dependent on the peptide length and on the position of tyrosine in the sequence.

Spectral Properties of the Purified Polymers. All the polymers obtained exhibited typical absorption and fluorescence properties already reported for polytyrosine (Gross & Sizer, 1959; Andersen, 1966), as shown in Table 2.

Kinetic Analysis of the Formation of the Polymer after Oxidation of Model Peptides. Using reverse phase chromatography, an analytical method was developed to simultaneously monitor the kinetics of monomer reaction along with polymer formation. Whatever the tyrosine carrier and the enzyme and substrate concentrations used, the consumption

Table 1: Amount of Tyrosine Contained in the Different Polymers Obtained after HRP Oxidation of Some Model Molecules Reported in the Percent of the Total Amount of Tyrosine Present in the Mixture at the Start[a]

	monomer	dimer	trimer	tetramer	polymers
L-tyrosine	20	17	nd	nd	63
NAT	14	47	30	7	2
py	23	38	35	4	0
pyp	72	28	0	0	0
pyq	77	23	0	0	0
yp	29	nd	nd	nd	71

[a] Values reported in the polymers column correspond to the amount of unidentified polymerization products. We failed to separate the different polymerization products obtained from the oxidation of *yp*. nd means not determined.

Table 2: Some Spectral Properties of the Polymerization Products Obtained after HRP Oxidation

	absorption maximum		ϵ_{max}		fluorescence (alkaline pH)
compound	acid	alkaline	acid	alkaline	emission maximum
py	276.4	293	1561	2994	310
$(py)_2$	287	318	5556	8667	407
$(py)_3$	290	326.2	10435	11900	407
NAT	274.5	293.5	1340	2330	310
$(NAT)_2$	286	318	4850	8300	407

of monomer never went to completion. Figure 3A illustrates the exceptionally low yield of $(pyp)_2$ generated (20% at best). In comparison, under the same conditions, the oxidation of *py* led to the polymerization of 77% of the total tyrosines. At least three possibilities may account for these observations. (i) The reaction reaches the thermodynamic equilibrium. This implies that HRP is able to catalyze the cleavage of the C−C bond cross-linking two aromatic rings. This hypothesis is unlikely. (ii) The enzyme may undergo an inactivation during the reaction. We have proceeded to Selwyn's test (Selwyn, 1965). Whatever the complexity of an enzyme reaction, the extent of reaction ξ is always proportional to the time and to the enzyme concentration. One can write

$$\xi = F[\mathrm{E}]t$$

where [E] is the concentration in active enzyme and t is time. F is a function of the instantaneous concentrations of the substrates, products, inhibitors, and any other species that may be present, but its exact form is not required. The convenience of this equation is that, if there is no appreciable inactivation of the enzyme during the time of observation, the graphs of ξ versus [E]t for different enzyme concentrations should be superimposable. The dimerization of *pyp* as a function of time is plotted for different HRP concentrations in Figure 3B. The kinetics are indeed superimposable. The enzyme is not inactivated within the time of observation. (iii) The products of the reaction may behave as inhibitors. A mechanism whereby the aromatic ring of the tyrosine molecule needs to be bound to the HRP prior to its oxidation may be postulated. As seen above, dimers and trimers are also substrates of the enzyme. They might compete with the monomers at the binding site of the enzyme. If their affinity for the enzyme is higher than the one of the monomers, and if their oxidation rate is slower, an abortive complex may form, decreasing the amount of free enzyme available. In order to test this hypothesis, the kinetics of

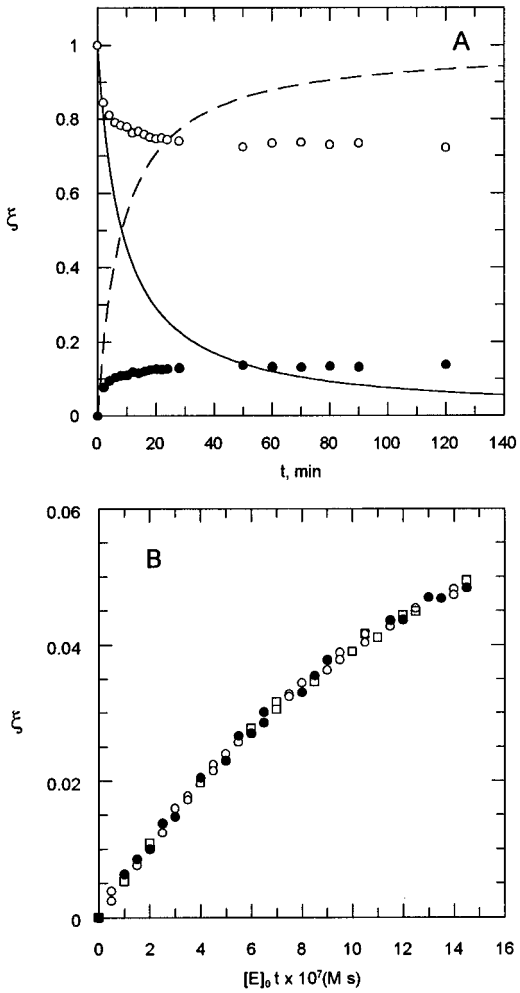

FIGURE 3: (A) Time courses for *pyp* monomer consumption (○) and $(pyp)_2$ dimer formation (●). Experimental conditions were the same as in Figure 2 except that the H_2O_2 concentration was 0.5 mM. The theoretical curves for the evolution of *pyp* and $(pyp)_2$ versus time have been calculated using the simple dimerization model

$$2pyp \xrightarrow{k} (pyp)_2$$

According to this scheme, monomer consumption is described by the equation $\xi = (pyp)_t/(pyp)_0 = 1/[1 + k(pyp)_0t]$ (solid line) and dimer formation by the equation $\xi = (pyp_2)_t/(pyp)_0 = 2[k(pyp)_0t/[1 + k(pyp)_0t]]$ (broken line). (B) Extent of *pyp* dimerization as a function of time for three HRP concentrations. The HRP concentrations were (○) 1 nM, (●) 2 nM, and (□) 10 nM, respectively, in 50 mM ammonium acetate (pH 8.7) containing 0.5 mM *py* and 0.5 mM H_2O_2.

polymerization of *py* were also analyzed after oxidation by the manganese-dependent peroxidase (MnP) from *P. chrysosporium*, another kind of enzyme which does not bind to the monomer prior to its oxidation. In the presence of organic acids such as lactic acid, Mn^{2+}, and H_2O_2, the MnP releases a lactate−Mn^{3+} complex which diffuses freely to the tyrosine aromatic ring and is able to oxidize it. MnP acts as a ''distant catalyst'', and as there is no direct binding of the aromatic compounds to the enzyme, the yield of polymerization should be higher. The comparisons of HRP and MnP mechanisms are shown in Figure 4. MnP and HRP catalyzed the *py* oxidation to give products that produced the same polymers. As shown in Figure 5, the behaviorial kinetics of the two enzymes were radically different. When the polymerization was catalyzed by the MnP, the reaction of the monomer was complete.

$$HRP + H_2O_2 \rightarrow CI$$

$$CI + R\text{-}Tyr \rightarrow CII + R\text{-}Tyr^{\bullet}$$

$$CII + R\text{-}Tyr \rightarrow HRP + R\text{-}Tyr^{\bullet}$$

$$2\ R\text{-}Tyr^{\bullet} \rightarrow (R\text{-}Tyr)_2$$

$$MnP + H_2O_2 \rightarrow CI$$

$$CI + Mn^{2+} + Lact \rightarrow CII + [Mn^{3+}\text{-}Lact]$$

$$CII + Mn^{2+} + Lact \rightarrow MnP + [Mn^{3+}\text{-}Lact]$$

$$2\ [Mn^{3+}\text{-}Lact] + 2\ R\text{-}Tyr \rightarrow 2\ R\text{-}Tyr^{\bullet} + 2\ Mn^{2+}$$

$$2\ R\text{-}Tyr^{\bullet} \rightarrow (R\text{-}Tyr)_2$$

(from Kuan et al. 1993)

FIGURE 4: Mechanisms for HRP- and MnP-catalyzed oxidation of tyrosine. The MnP tyrosine oxidation mechanism is derived from the general MnP mechanism postulated by Kuan et al. (1993): CI, compound I; CII, compound II.

Steady State Kinetics of py Oxidation. The classic reaction scheme for HRP (see Figure 4) does not include a Michaelis−Menten-like adsorption complex between the enzyme and donor. According to this scheme, the mechanism should not be rate-limiting at high donor concentrations (Brill, 1966). However, one cannot ignore the possibility of saturating action of the enzyme by the donor. Data suggested it was possible to saturate the HRP with at least three of the tested substrates. A saturation of the HRP was observed for *py* concentrations on the order of 15 mM (Figure 6A). The apparent K_M for this donor was 2.1 ± 0.3 mM, and V_m^{app} = 14 ± 0.04 μM/min ($k_{cat} \approx 58\ s^{-1}$). When the dimeric form of NAT [$(NAT)_2$] was present in the reaction mixture, a decrease of the initial rate (v_0) was observed. The graphical representations of the Hanes equation (Cornish-Bowden, 1979) were plotted for several concentrations of $(NAT)_2$ with a constant value being obtained for the slopes ($1/V_m^{app}$) (Figure 6B). This behavior resembled competitive inhibition of the reaction by $(NAT)_2$. The apparent K_I of $(NAT)_2$ was 18 ± 0.13 μM. Saturation phenomena of HRP were also observed with NAT and Gly-Tyr (data not shown).

Determination of the True Second-Order Constants k_2 and k_3 of Tyrosine Oxidation Catalyzed by CI and CII Forms of HRP. In order to compare the true second-order constants k_2 and k_3, single-turnover experiments were performed with a stopped flow apparatus. According to the scheme above, the enzyme is converted to a compound I intermediate (CI) upon oxidation by hydrogen peroxide. When the first donor molecule is oxidized, compound I is reduced to compound II (CII). This step is accompanied by an increase in the absorption of the enzyme at 422 nm. Upon the oxidation of a second molecule of donor, the enzyme returns to its ''resting state''. This reduction is accompanied by a decrease of the absorption at 422 nm. The data for HRP reduction with *py* or L-tyrosine as donors are shown in Figure 7. We have assumed that the step involving free radical condensation leading to the polymerization was not rate-limiting.

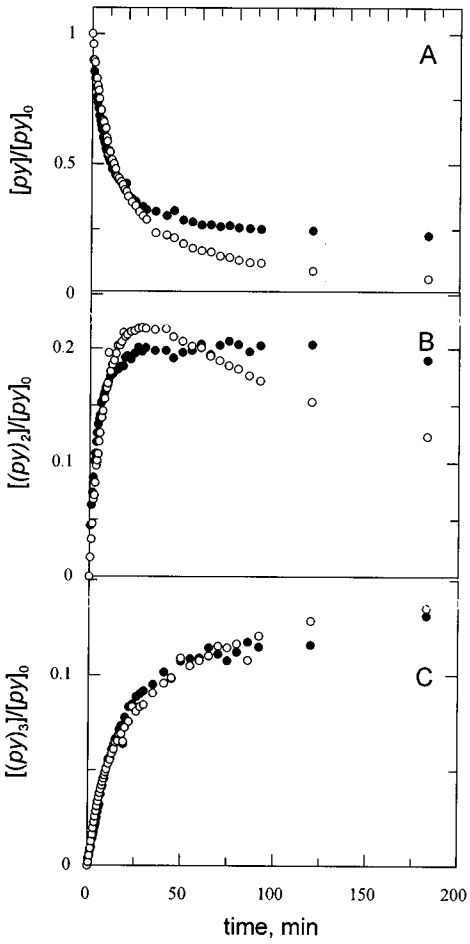

FIGURE 5: Time courses for *py* consumption (A) and for $(py)_2$ (B) and $(py)_3$ (C) formation. When HRP was used (●), the mixture contained 0.3 mM *py* and 0.6 μM enzyme in 50 mM ammonium acetate (pH 8.7). When MnP was used (○), the mixture contained 0.3 mM *py* and 5 μM enzyme in 50 mM sodium lactate (pH 4.5) containing 0.1 mM $MnSO_4$. The reactions were initiated by addition of 2 mM H_2O_2. Aliquots (100 μL) were withdrawn every minute and analyzed as described in Materials and Methods.

According to this, the k_4' constant determined from the kinetics of polymer formation (see Materials and Methods) should reflect the oxidation steps of the tyrosine residues catalyzed by the enzyme. Table 3 summarizes the values of the different constants obtained by means of steady state measurements and stopped flow techniques. The data show that the discrepancies observed between the polymerization rates of the different donor substrates studied were conditioned by the steps of enzymatic oxidations (mainly the step of CII reduction to the resting enzyme, as k_3 and k_4' have very close values).

DISCUSSION

We have shown that the oxidation by HRP of the tyrosine-containing peptides is accompanied by their limited polymerization, as shown in Table 1. One reason for this limitation is almost certainly steric hindrance, which probably prevents higher degrees of polymerization. However, it was demonstrated in this study that the polymerization is also limited, due to enzyme inhibition by the polymers themselves. The inhibitory effect obtained with $(NAT)_2$ has been quantified (K_I = 20 μM). This effect was not observed when the oxidation was catalyzed by MnP. In this situation, the oxidation of the aromatic donor proceeds at a distance via the intermediate complex lactate−Mn^{3+} released by MnP,

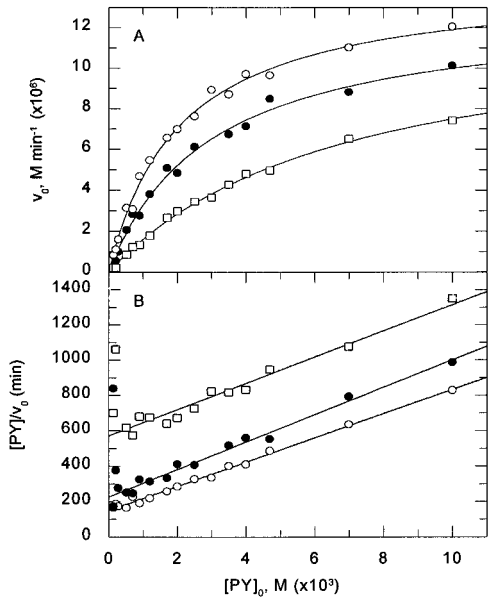

FIGURE 6: Effect of dimer $(NAT)_2$ on the initial rate of *py* polymerization. Initial rate (A) of *py* polymerization plotted as a function of *py* initial concentration. Experiments were carried out in 50 mM phosphate buffer (pH 8.7) containing 5 nM HRP and 100 μM H_2O_2. $(NAT)_2$ concentrations were 0 μM (○), 20 μM (●), and 50 μM (□). Hanes equation (B) graphical representation ([*py*]/v_0 versus [*py*]).

and there is no complex formation between enzyme and donor (i.e. tyrosine residue) prior to its oxidation.

For several substrates (*py*, NAT, and Gly-Tyr), saturation of HRP was achieved. Therefore, it is necessary to consider the fact that the enzyme is able to form an adsorption complex with the donors. Although there is no doubt that this type of intermediate exists physically [for review, see Dunford (1991)], until now, it had never been necessary to take this into account to explain the kinetic behavior of HRP (Chance, 1951). For all the substrates which have been tested, the dimerization rate constant k'_4 reflects k_3, the magnitude of the rate constant of tyrosine oxidation by CII (Table 3). Consequently, it was possible to confirm that the free radical condensation was not the limiting step of the mechanism but that CII reduction to the resting enzyme was the controlling factor. Thus, experimental determination of k'_4 at appropriate donor and H_2O_2 concentrations gives a good approximation of k_3. For saturating substrates, a pseudo-first-order rate constant, $k'_{4_{cal}}$, of dimerization was calculated from the steady state kinetic parameters K_M^{app} and k_{cat}. At low substrate concentrations, $[R-Tyr]_0 \ll K_M^{app}$. One can write

$$v_0 = \frac{k_{cat}[E]_{tot}[R-Tyr]_0}{K_M^{app}}$$

and

$$k'_{4_{cal}} \approx \frac{k_{cat}}{K_M^{app}}$$

with k_{cat} being the catalytic constant. The calculated constants were in good agreement with the experimental k'_4 (steady state) and k_3 (fast kinetic) values. It was also shown that dimers behave as competitive inhibitors toward oxidation of monomers. However, dimers cannot be considered "true"

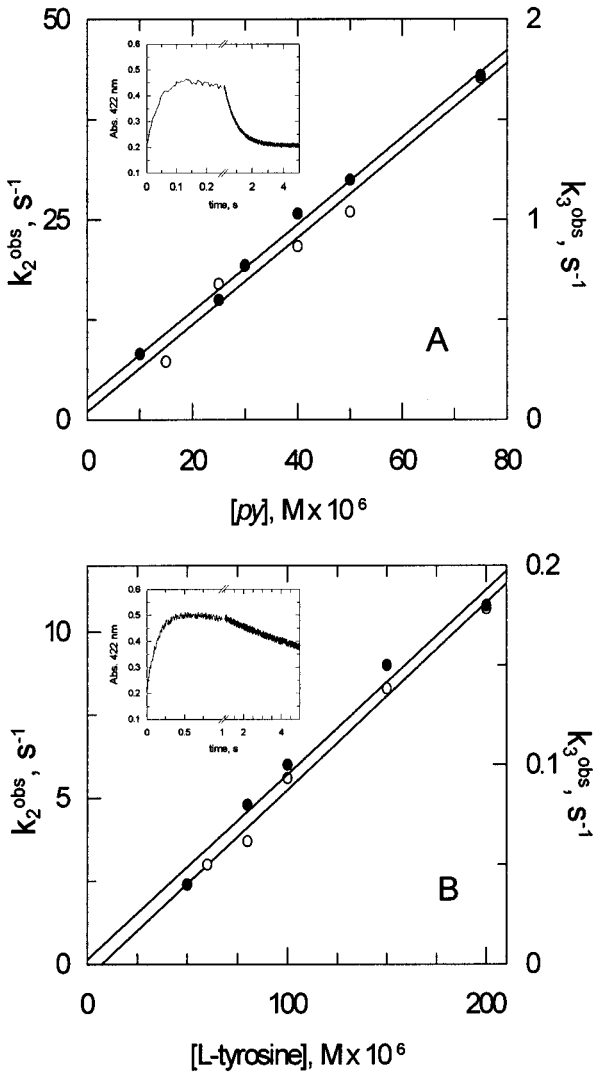

FIGURE 7: Pseudo-first-order rate constants of HRP reduction as a function of donor concentration. (○) k_2^{obs} and (●) k_3^{obs} are respectively the pseudo-first-order rate constants of reduction of compound I to compound II and of compound II to the resting enzyme using (A) *py* and (B) L-tyrosine as the electron donor. (Insets) Time courses for compound I reduction to compound II (absorbance increase) and compound II reduction to the resting HRP (absorbance decrease) using *py* (A) and L-tyrosine (B) as donors. HRP (4 μM) was preincubated with an equimolar concentration of H_2O_2 prior to mixing with 50 μM *py* or 150 μM L-tyrosine in 50 mM phosphate buffer at pH 7.14 and 25 °C.

inhibitors since several of them are oxidized to form larger polymers [$(py)_3$, $(NAT)_3$, and $(NAT)_4$]. In order to interpret these observations, one can propose the following simplified scheme:

$$\text{CII} + \text{R–Tyr} \xleftrightarrow{K_s} \text{CII•R–Tyr} \xrightarrow{k_3^{R-Tyr}} \text{E} + \text{R–Tyr}^\bullet$$

$$\text{CII} + (\text{R–Tyr})_2 \xleftrightarrow{K_I} (\text{CII•(R–Tyr)}_2) \xrightarrow{k_3^{(R-Tyr)2}} \text{E} + (\text{R–Tyr})_2^\bullet$$

$$\left.\begin{array}{l} 2\text{R–Tyr}^\bullet \\ \text{R–Tyr}^\bullet + (\text{R–Tyr})_2^\bullet \\ 2(\text{R–Tyr})_2^\bullet \end{array}\right\} \xrightarrow{k_4} \left\{\begin{array}{l} (\text{R–Tyr})_2 \\ (\text{R–Tyr})_3 \\ (\text{R–Tyr})_4 \end{array}\right.$$

where $K_s \gg K_I$ and $k_3^{R-Tyr} \gg k_3^{(R-Tyr)_2}$. It must be emphasized that this scheme only takes into account the rate-limiting step (i.e. CII reduction to the resting enzyme) governing the initial steady state velocity (see above).

Table 3: Kinetic Parameters for the Oxidation of Tyrosines Contained in Various Model Compounds[a]

substrate	k_{cat} (s^{-1})	K^{app}_M ($M \times 10^3$)	k'_4 ($M^{-1}\ s^{-1}$) measured	k'_4 ($M^{-1}\ s^{-1}$) calculated	k_2 ($M^{-1}\ s^{-1}$)	k_3 ($M^{-1}\ s^{-1}$)	notes[b]
L-Tyr	ns	ns	821	nd	56 000	1016	this study
			753	nd			1
					50 000		2
						2000	3
$(Tyr)_2$	nd	nd		nd	112 000	750	4
NAT	94	5.6	17800	16786	252 174	19398	this study
$(NAT)_2$	nd	nd	913	nd	17 476	1028	this study
NATA	ns	ns	17698	nd	241 000	23000	this study
Gly-Tyr	175	10.8	17116	16203	nd	nd	this study
py	58	2.1	24700	29166	516 000	21600	this study

[a] nd means not determined; ns means no saturation obtained in the range of solubility. k'_4 was determined experimentaly (see Materials and Methods) or calculated using steady state parameters in cases where substrate saturation was obtained using the approximation $k'_4 \approx k_{cat}/K^{app}_M$ at low substrate concentrations. [b] The references were as follows: (1) Bayse et al. (1972), (2) Ralston and Dunford (1978), (3) Ralston and Dunford (1980), and (4) Marquez and Dunford (1995).

Hence, it is possible to define k_{on} and k_{off} as follows

$$CII + R{-}Tyr \underset{k_{off}}{\overset{k_{on}}{\rightleftharpoons}} (CII{\cdot}R{-}Tyr)$$

One can also write

$$K^{app}_M = \frac{k_{off} + k_{cat}}{k_{on}} = K_s + \frac{k_{cat}}{k_{on}}$$

The association rate constant of the enzyme and donor (k_{on}) is generally on the order of $10^9\ s^{-1}\ M^{-1}$ (when closed to the diffusion-controlled encounter frequency) and $10^6\ s^{-1}\ M^{-1}$ (when several steps occur during association) (Ferscht, 1985). Using the above relationship, one can estimate that, for *py* ($k_{cat} = 58\ s^{-1}$), K^{app}_M is close to K_s whatever the k_{on} value between 10^6 and $10^9\ s^{-1}\ M^{-1}$. The affinity of $(NAT)_2$ for HRP is hence 100 times higher then the one of *py* (as $K_I = 20\ \mu M$ and $K_s \approx K^{app}_M = 2$ mM). It is also necessary to validate the assumption $k_3^{R-Tyr} \gg k_3^{(R-Tyr)_2}$.

The k'_4 values obtained for $(NAT)_2$ and *py* are 913 and 24 700 $M^{-1}\ s^{-1}$, respectively. These values are in good agreement with the ones obtained using stopped flow techniques [$k_3^{py} = 21\ 600\ M^{-1}\ s^{-1}$ and $k_3^{(NAT)_2} = 1028\ M^{-1}\ s^{-1}$]. The dimers exhibit a higher affinity for the enzyme than the monomers. During the full extent of reaction, these dimers progressively displace an increasing amount of free enzyme toward the formation of the enzyme−dimer complex. The oxidation of dimers was 20 times slower then the oxidation of monomers [see above for $k_3^{(NAT)2}$ and k_3^{py} values], and the dimers display an inhibitory effect related to competitive inhibition. To summarize, we propose a model which involves an adsorption complex formed between HRP and the donor. A pseudo-first-order rate constant (k'_4) of dimerization was calculated from the steady state kinetic parameters K^{app}_M and k_{cat}. This constant was in good agreement with the one of the limiting step

$$CII + R{-}Tyr \xrightarrow{k_3} E + R{-}Tyr^{\bullet}$$

suggested in Chance (1943). Therefore, it is clear that the two models are not mutually exclusive. In effect, they describe the behavior of the system for different donor concentration ranges.

The values of the second-order rate constants k_2 and k_3 obtained for L-tyrosine oxidation are in agreement with the ones previously reported (Ralston & Dunford, 1978, 1980). NAT and NATA are closely related structurally to L-tyrosine, but the k_2 and k_3 values of their oxidation by CI and CII are 5 and 20 times higher, respectively, than the ones of L-tyrosine (see Table 3). At the pH values of the samples in the experiments (between 7.2 and 8.7), all substrates with the exception of NATA carry a negative charge on the terminal carboxyl group. Therefore, this group does not seem to be involved in the observed discrepancies. Thus, the rate constants may depend on the positive ionization of the α-amino group as NAT and NATA are devoid of a free amino group. Moreover, the relative positions of the amino group and of the aromatic ring carried by the tyrosine side chain may have an effect as the oxidation of Gly-Tyr is more efficient than the oxidation of tyrosine alone. *py* was the best substrate tested. However, for this latter one, the positive charge carried by the N-terminal proline is located far from the aromatic ring. Hence, a decrease was observed in the rate of L-tyrosine oxidation by CII when this residue was positively charged. Our observations are not in accordance with previous results showing that the rate of oxidation of L-tyrosine by the CII compound of HRP decreases above pH 9 (Ralston & Dunford, 1980). The half-effect observed corresponded to a pK_a of 9.16 and was attributed by these authors to proton release either from the α-amino group of the tyrosine or from an acidic group on the enzyme. Therefore, our findings are in better agreement with their second hypothesis. This last hypothesis was supported elsewhere by the fact that the CII oxidation of paracresol, which is a neutral aromatic compound structurally related to the L-tyrosine side chain, exhibits an enzymatic pK_a of 8.6 (Critchlow & Dunford, 1972).

It has been previously reported that k_2, the rate of reduction of CI to CII by L-tyrosine, increases with the deprotonation of the tyrosine amino group (Ralston & Dunford, 1978). The role of Arg 38 in CI formation (Dunford, 1991) might be affected by the presence of a positive charge carried by the donor. This effect should not be observed with neutral amines (NAT and NATA) or for substrates carrying charges located far enough from the aromatic ring (Gly-Tyr and *py*). One may argue that CI should be formed before the donor can be bound. Despite this assertion, several studies have shown that donors bind to the resting enzyme (Schejter et al., 1976; Critchlow & Dunford, 1972; Adak et al., 1996). Moreover, Childs and Bardsley (1975) have pointed out that for relatively high donor concentrations the binding of the donor to the free enzyme prior to its conversion to CI by

H_2O_2 should not be excluded. Finally, the affinities of the donor for the resting enzyme and for its peroxidative form are probably different.

It has also been reported that there is a linear dependence between tyrosine concentration and its subsequent oxidation rate (Bayse et al., 1972; Ralston & Dunford, 1980) up to a concentration of 2 mM tyrosine. It is our belief that the tyrosine concentrations required for saturating HRP are far beyond the limit of its solubility. Attempts to estimate the K_M^{app} of tyrosine have been made by performing steady state kinetic measurements at pH 10, the phenolate form of tyrosine being more soluble than its phenolic form. The value of this parameter is probably in excess of 40 mM. In a recent work, it was reported that myeloperoxidase from mammalian sources cannot be saturated by tyrosine (Marquez & Dunford, 1995) within the solubility domain of this substrate. A K_M value of 300 μM was reported for the oxidation of L-tyrosine catalyzed by rat intestinal peroxidase (Valoti et al., 1992). The concentration range used by these authors to determine this value was rather narrow (between 100 and 250 μM), but one cannot exclude the fact that this enzyme exhibits different properties than HRP. Saturation has been obtained for NAT, *py*, and Gly-Tyr. These substrates are all devoid of positive charges close to the aromatic ring of the tyrosine side chain. The positive charge of tyrosine may decrease its affinity for the enzyme. Arg 183 is probably involved in the binding of the aromatic donors to the HRP prior to their oxidation (Adak et al., 1996). At the pH values of our measurements, this arginine was protonated. A possible repulsive effect between Arg 183 and the amino group of the tyrosine may be the cause of the relatively low affinity of tyrosine for HRP.

In vivo, the efficiency of the peroxidase oxidation of proteins probably depends on the vicinity of target tyrosines (Fry, 1982). We have shown that the presence of positive charges in close proximity to the aromatic ring decreases the activity of the enzyme. It was also observed that the rate constant of *py* oxidation is twice that determined for the oxidation of the other model peptides. It is possible that some elements of the peptide structure define specific oxidation sites on the proteins. We have shown that dimers exhibit higher affinities for HRP than tyrosine. Conversely, their rate of oxidation by CII compounds is weaker. The CII compound of phagocytary myeloperoxidase also oxidizes dityrosine at a lower rate than L-tyrosine (Marquez & Dunford, 1995). *In vivo*, myeloperoxidase is responsible for the oxidative cross-linking of lipoproteins (Winterbourn, 1992). This cross-linking should occur through dityrosine condensation. The oxidized lipoproteins are involved in the formation of atherosclerotic plaques. Recently, a study has shown that, *in vitro*, lipoproteins seem to be more efficiently oxidized by hemoglobin than by HRP (Miller et al., 1996). The binding of peroxidases to dityrosines formed already should prevent further enzyme-catalyzed oxidations. One should consider that, in addition to an oxidative stress, a local increase in the dityrosine concentration induces a complexation of the CII compound, thus producing a decrease of the pool of active peroxidases.

ACKNOWLEDGMENT

We thank Anitra Rabesona for peptide synthesis, Eric Ferrasson and Weichi Wang for their technical assistance, and Daniel Mollet for mass spectroscopy analysis. We are gratful to Dipak Sarker for kindly reviewing the English of the manuscript.

REFERENCES

Adak, S., Mazmumder, A., & Banerjee, R. K. (1996) *Biochem. J. 314*, 985−991.
Amado, R., Aeschbach, R., & Neukom, H. (1984) *Methods Enzymol. 107*, 377−388.
Andersen, S. O. (1966) *Acta Physiol. Scand. 66* (Suppl.), 263.
Asther, M., Vilter, H., Kurek, B., & Meunier, J. C. (1992) *Int. J. Biochem. 24*, 1377−1383.
Bayse, G. S., Michaels, A. W., & Morrison, M. (1972) *Biochim. Biophys. Acta 284*, 34−42.
Bidlingmeyer, B. A., Cohen, S. A., & Tarvin, T. L. (1984) *J. Biochem. 336*, 93−104.
Brill, A. S. (1966) *Compr. Biochem. 14*, 447−477.
Capdevila, C., Corrieu, G., & Asther, M. (1989) *J. Ferment Technol. 68*, 60−63.
Chance, B. (1943) *J. Biol. Chem., 151*, 553−567.
Chance, B. (1951) *Adv. Enzymol. 12*, 153−190.
Childs, R. E., & Bardsley, W. G. (1975) *Biochem. J. 145*, 93−103.
Cornish-Bowden, A. (1979) in *Fundamentals of Enzyme Kinetics*, pp 26−27, Butterworth & Co. Ltd., Kent, U.K.
Critchlow, J. E., & Dunford, H. B. (1972) *J. Biol. Chem. 247*, 3703−3713.
Dunford, H. B. (1991) in *Peroxidases in Chemistry and Biology* (Everse, J., Everse, K. E., & Gresham, M. B., Eds.) Vol. 2, pp 1−24, CRC Press, Boca Raton, FL.
Federico, R., & Angelini, R. (1986) *Planta 167*, 300−302.
Fersht, A. (1985) in *Enzyme Structure and Mechanism*, pp 150−151, W. H. Freeman and Company, New York.
Fry, S. F. (1982) *Biochem. J. 204*, 449−455.
Glenn, J. K., & Gold, M. H. (1985) *Arch. Biochem. Biophys. 242*, 329−341.
Gross, A. J., & Sizer, I. W. (1959) *J. Biol. Chem. 234*, 1611−1614.
Job, D., & Dunford, H. B. (1978) *Can. J. Biochem. 56*, 1327−1334.
Kieliszewski, M. J., & Lamport, D. T. A. (1994) *Plant J. 5*, 157−172.
Kirk, T. K., Croan, S., & Tien, M. (1986) *Enzyme Microb. Technol. 8*, 27−32.
Kuan, I., Johnson, K. A., & Tien, M. (1993) *J. Biol. Chem. 268*, 20064−20070.
LaBella, F., Keeley, F., Vivian, S., & Thornhill, D. (1967) *Biochem. Biophys. Res. Commun. 26*, 748−753.
Malencik, D. A., & Anderson, S. R. (1996) *Biochemistry 35*, 4375−4386.
Marquez, A. M., & Dunford, H. B. (1995) *J. Biol. Chem. 270*, 30434−30440.
Miller, Y. I., Felikman, Y., & Shaklai, N. (1996) *Arch. Biochem. Biophys. 326*, 252−260.
Millis, C. D., Cai, D., Stankovich, M., & Tien, M. (1989) *Biochemistry 28*, 8484−8489.
Press, W. H., Flannery, B. P., Teukolsky, S. K., & Vetterling, W. T. (1986) in *Numerical Recipes*, Cambridge University Press, Cambridge.
Ralston, I. M., & Dunford, H. B. (1978) *Can. J. Biochem. 56*, 1115−1119.
Ralston, I. M., & Dunford, H. B. (1980) *Can. J. Biochem. 58*, 1270−1276.
Scalet, M., Federico, R., & Angelini, R. (1991) *J. Plant Physiol. 137*, 571−575.
Schejter, A., Lanir, A., & Epstein, N. (1976) *Arch. Biochem. Biophys. 174*, 36−44.
Selwyn, M. J. (1965) *Biochim. Biophys. Acta 105*, 193−195.
Valoti, M., Tipton, K. F., & Sgaragli, P. (1992) *Biochem. Pharmacol. 43*, 945−951.
Winterbourn, C. C., Vandenberg, J. J. M., Roitman, E., & Kuypers, F. A. (1992) *Arch. Biochem. Biophys. 296*, 547−555.

BI963168Z